Modeling Alveolar Soft Part Sarcoma Unveils Novel Mechanisms of Metastasis

Article *in* Cancer Research · December 2016

DOI: 10.1158/0008-5472.CAN-16-2486

6 authors, including:

Miwa Tanaka
Japanese Foundation for Cancer Research
23 PUBLICATIONS **350** CITATIONS
SEE PROFILE

Takuro Nakamura
University Hospital Medical Information Net…
107 PUBLICATIONS **3,791** CITATIONS
SEE PROFILE

Published OnlineFirst December 15, 2016; DOI: 10.1158/0008-5472.CAN-16-2486

Molecular and Cellular Pathobiology

Cancer Research

Modeling Alveolar Soft Part Sarcoma Unveils Novel Mechanisms of Metastasis

Miwa Tanaka[1], Mizuki Homme[1], Yukari Yamazaki[1], Rikuka Shimizu[1], Yutaka Takazawa[2], and Takuro Nakamura[1]

Abstract

Alveolar soft part sarcoma (ASPS) is a slowly growing, but highly metastatic, sarcoma that affects adolescents and young adults. Its characteristic alveolar structure is constituted by tumor cell nests and an abundant vascular network that is responsible for metastatic activities at the initial stage. Here, we have generated a new *ex vivo* mouse model for ASPS that well recapitulates associated angiogenic and metastatic phenotypes. In mouse ASPS, the tumor cells frequently showed tumor intravasation, with the intravascular tumor cells presenting as organoid structures covered with hemangiopericytes, which is also observed in human ASPS. High expression of glycoprotein nmb (GPNMB), a transcriptional target of ASPSCR1-TFE3, was observed at the sites of intravasation. ASPS tumor cells also demonstrated enhanced transendothelial migration activity, which was inhibited by silencing of *Gpnmb*, indicating that GPNMB plays an important role in tumor intravasation, a key step in cancer metastasis. The present model also enabled the evaluation of TFE/MITF family transcription factor function, which demonstrated that ASPSCR1-TFEB possessed definitive albeit less marked oncogenic activity than that of ASPSCR1-TFE3. Collectively, our mouse model provides a tool to understand oncogenic, angiogenic, and metastatic mechanisms of ASPS. It also identifies important motifs within the ASPSCR1-TFE3 fusion protein and provides a platform for developing novel therapeutic strategies for this disorder. *Cancer Res; 77(4); 897–907. ©2016 AACR.*

Introduction

Alveolar soft part sarcoma (ASPS) is a soft-tissue sarcoma affecting adolescents and young adults between 15 and 35 years of age, which is characterized by frequent hematogenous metastases even prior to primary hospital admission (1). The most frequent location of the primary ASPS consists of the deep muscles of the lower extremities; however, the cell of origin remains unidentified (2). Although ASPS represents a slowly growing sarcoma, its prognosis is unfavorable with a survival rate of 60% at 5 years (2, 3). The *ASPSCR1-TFE3* fusion gene generated by chromosomal translocation t(X;17)(p11.2;q25) is causally associated with ASPS with the resultant protein modulating its target genes as an oncogenic transcription factor via a DNA-binding motif derived from TFE3 (4–7).

ASPS has a characteristic alveolar structures of tumor cells separated by thin fibrous septa and a delicate but highly integrative vascular network (2). The abundance of blood vessels causes frequent intravasation of tumor cells, correlated with the high metastatic potential. An upregulation of a series of angiogenesis-related genes has been reported in ASPS (8); however, the mechanisms of modulation in gene expression mediated by ASPSCR1-TFE3 as well as of key target molecules in ASPS vasculogenesis remains to be addressed. Toward this end, the establishment of a reliable animal model that is useful in understanding the tumorigenic and vasculogenic mechanisms of human ASPS is desired.

It has recently been reported that conditional *ASPSCR1-TFE3* expression in the mouse resulted in ASPS-like sarcoma (9). In the model, ASPS mainly occurred as intracranial tumors, although, unlike human ASPS, metastatic features were not exhibited. In contrast, in the current study, we present a novel mouse model for ASPS generated using an *ex vivo*–based technology previously utilized in generation of an Ewing sarcoma model (10). The present model well recapitulates the pathologic and biological features of human ASPS and provides important information toward understanding the mechanisms of vasculogenesis and metastasis.

Materials and Methods

Plasmid construction

N-terminal FLAG-tagged *ASPSCR1-TFE3* was introduced into both the pMYs-IRES-GFP and pMYs-IRES-Luc vectors. The full-length *ASPSCR1-TFE3* was cloned from a human ASPS case. Artificial chimeric *ASPSCR1* fusions between *ASPSCR1* and *TFEB*, *TFEC*, or *MITF* were also generated by two-step PCR using primers encompassing both *ASPSCR1* and *TFE* family genes, and in-frame fusions were confirmed by sequencing. The FLAG-tagged full-length coding sequences of each fusion genes were subcloned into the pMYs retroviral vector, and protein expression and nuclear localization were confirmed by Western blotting and immunofluorescence, respectively (Supplementary Fig. S3). cDNA clones

[1]Division of Carcinogenesis, The Cancer Institute, Japanese Foundation for Cancer Research, Tokyo, Japan. [2]Division of Pathology, The Cancer Institute, Japanese Foundation for Cancer Research, Tokyo, Japan.

Note: Supplementary data for this article are available at Cancer Research Online (http://cancerres.aacrjournals.org/).

Corresponding Author: Takuro Nakamura, The Cancer Institute, Japanese Foundation for Cancer Research, 3-8-31 Ariake, Koto-ku, Tokyo 135-8550, Japan. Phone: 81-3-3570-0462; Fax: 81-3-3570-0463; E-mail: takuro-ind@umin.net

doi: 10.1158/0008-5472.CAN-16-2486

Published OnlineFirst December 15, 2016; DOI: 10.1158/0008-5472.CAN-16-2486

spanning the entire coding regions of human *TFEB*, *TFEC*, and *MITF* were purchased from Dnaform.

Generation and characterization of the ASPS model mouse

Extremities of Balb/c mouse embryos (Clea Japan) were removed aseptically on 18.5 dpc, and then dissected using 2 mg/mL collagenase (Wako Pure Chemical) at 37°C for 2 hours. Retroviral infection of embryonic mesenchymal cells (eMC) and their transplantation into the subcutaneous regions of Balb/c nude mice were performed as described previously (10). The mice were observed daily to check for tumor formation and general condition, and tumors were resected and subjected to further examination when subcutaneous masses reached 15 mm in diameter as described previously (10). The GFP transgenic (tg) mouse (11) was kindly provided by Dr. Masato Ikawa, and the mouse was subsequently backcrossed to the Balb/c strain to enable the receipt of Balb/c-derived ASPS cells. All experiments described in this study were performed in strict accordance with standard ethical guidelines and approved by the animal care committee at the Japanese Foundation for Cancer Research under licenses 10-05-9 and 0604-3-13.

Human ASPS specimens

Paraffin blocks from 14 cases of ASPS surgical specimens were obtained from The Cancer Institute Hospital. Informed consent was obtained from the donors, and the study was approved by the Institutional Review Board at Japanese Foundation for Cancer Research under license 2013-1155.

Histopathology and immunohistochemistry

For light microscopic analysis, formaldehyde-fixed, paraffin-embedded tumor tissues were stained with hematoxylin and eosin (H&E) using standard techniques. The ASPSCR1-TFE3 antigen was detected using a monoclonal mouse anti-FLAG antibody (M2; Sigma) in conjunction with the Histofine Simple Stain Kit (Nichirei). The following primary antibodies were used: anti-GPNMB (R & D Systems), anti–α-smooth muscle actin (aSMA; DAKO), anti-mouse PDGFRB (R & D Systems), anti-human PDGFRB (Santa Cruz Biotechnology), anti-mouse CD31 (Becton Dickinson), anti-mouse CD105 (Becton Dickinson), anti-human CD31 (DAKO), and anti-human CD34 (DAKO). For elextron microscopic observation, glutaraldehyde-fixed tumor tissues were embedded in epoxy resin, and ultra-thin sections were observed using a transmission electron microscope (H-7600; Hitachi).

Transendothelial migration assay

Mouse ASPS cell lines were established from subcutaneous tumors and maintained in Iscove's modified Dulbecco's medium (Invitrogen) supplemented with 10% FBS. Murine endothelial cells were isolated from 18.5 dpc Balb/c embryos as a CD31-positive, CD105-positive, and PDGFRB-negative fraction according to the previously reported criteria (12), and immortalized through transfection of the SV40 large T antigen. Transendothelial migration assays were carried out according to the previously reported method (13) with modification. Briefly, 6×10^5 of endothelial cells were seeded onto Boyden chambers containing Matrigel (Becton Dickinson) in a 24-well plate and then subjected to 20-Gy irradiation (CP160, Faxitron X-ray). Next, 5×10^5 ASPS or mouse Ewing sarcoma (10) cells were seeded onto the chambers, and the number of migrated cells was counted 24 hours after seeding. For knockdown of Gpnmb, siRNAs were purchased from Invitrogen (MSS294588 and MSS234870). siRNAs were introduced into ASPS cells using Lipofectamine 2000 (Life Technologies), and knockdown efficiencies were confirmed by Western blotting.

RT-PCR and real-time quantitative RT-PCR

Total RNA extraction, reverse transcription, and RNA quantification were performed according to methods described previously (14). Conventional RT-PCR and real-time quantitative RT-PCR were performed using a Gene Amp 9700 thermal cycler (Applied Biosystems) and a 7500 Fast Real-Time PCR System (Applied Biosystems), respectively. The sequences of the oligonucleotide primers used are shown in Supplementary Table S1.

Microarray analysis

GeneChip analysis was conducted to determine gene expression profiles. The murine HT MG-430 PM array (Affymetrix) was hybridized with aRNA probes generated from eMCs 48 hours after transduction with pMYs-*ASPSCR1-TFE3* or empty vector, ASPS tumor tissues, or a mixture of mouse normal tissues according to methods described previously (15). The expression data were analyzed using GeneSpring ver 12.6 (Agilent Technologies), and gene set enrichment analysis (GSEA) was performed using GSEA-P 2.0 software (16). The important signaling pathways were examined and illustrated by using the Ingenuity Pathway Analysis (IPA) software. The microarray data sets are accessible through the NCBI Gene Expression Omnibus database (http://www.ncbi.nlm.nih.gov/geo), with an accession number GSE86502.

Western blotting

Western blot analysis was performed using whole-cell lysates as described previously (14).

Statistical analysis

All data are given as the mean ± SEM. Survival analysis was performed using the Kaplan–Meier life table method, and survival between groups was compared with the log-rank test. Continuous distributions were compared with a two-tailed Student *t* test.

Results

Generation and characterization of the ASPS *ex vivo* model

In a previous study, we succeeded in generating a mouse model for Ewing sarcoma by the transduction of mouse embryonic osteochondrogenic progenitors with an *EWS-ETS* retrovirus (10). This result suggests that eMCs may also contain cellular compartments that are responsive to the products of oncogenic fusion genes in human sarcomas. Therefore, we introduced *ASPSCR1-TFE3* into murine eMCs derived from embryo extremities on dpc 18.5. We then injected 1×10^6 transduced cells subcutaneously into nude mice (Supplementary Fig. S1A). Recipient mice developed a subcutaneous mass at 100% penetrance with a mean latency of 17.5 weeks (Fig. 1A). In contrast, no tumor was developed by 15 months after transplantation when adult mesenchymal cells expressing *ASPSCR1-TFE3* were introduced (data not shown). Furthermore, abundant blood vessels surrounding the tumor mass were observed (Fig. 1B).

Published OnlineFirst December 15, 2016; DOI: 10.1158/0008-5472.CAN-16-2486

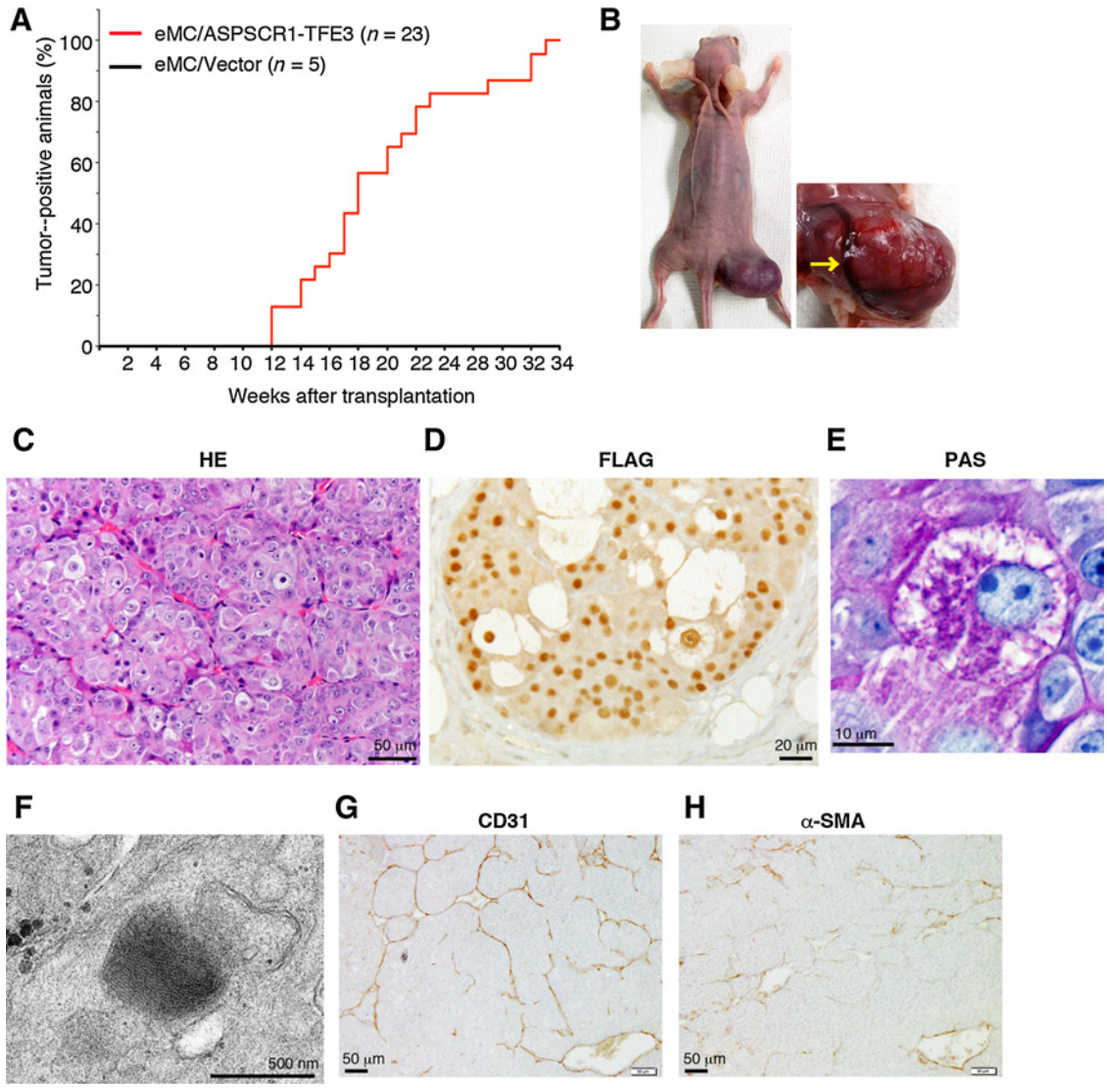

Figure 1.

The ASPS *ex vivo* model. **A,** Cumulative incidence of ASPS tumors induced by eMCs expressing ASPSCR1-TFE3 or containing an empty vector. **B,** Tumors could be observed as subcutaneous masses in recipient nude mice (left), and thick blood vessels (arrow) developed on the tumor surface (right). **C–E,** Histology of murine ASPS. H&E staining (**C**), immunostaining for anti-FLAG (**D**), and periodic acid–Schiff staining (**E**). **F,** Electron microscopy of the intracytoplasmic crystal structure of ASPS tumor cells. **G** and **H,** Immunohistological analysis of tumor vasculature in murine ASPS. Positive staining for the endothelial marker CD31 (**G**) and for the hemangiopericyte marker αSMA (**H**).

Histologic analysis showed that tumors expressing ASPSCR1-TFE3 were composed of organoid nests of polygonal to round tumor cells (Fig. 1C). The nuclei were also round, included prominent nucleoli, and were positive for FLAG-tagged ASPSCR1-TFE3 (Fig. 1D). Notably, intracytoplasmic periodic acid–Schiff-positive rod-shaped crystals were observed (Fig. 1E), which represents a characteristic feature of human ASPS (1, 3). The distinct crystal structures were also observed by electron microscopic analysis (Fig. 1F). Cytoplasmic mitochondria and lysosomes were also abundant in ASPS cells (Supplementary Fig. S1B), and fibrovascular septa and delicate capillary blood vessels were also prominent in mouse ASPS tumors. These blood vessels were positive for the endothelial marker CD31 (Fig. 1G) as well as for the hemangiopericyte markers aSMA and PDGFRB (Fig. 1H; Supplementary Fig. S1C).

Metastatic potentials and vascular structure of ASPS

In our ASPS model, 52.2% (12 of 23) mice with tumors showed multiple metastatic foci in the lungs (Fig. 2A). The high metastatic incidence from subcutaneous tumors reflects the character of human ASPS and suggests the strong induction of vasculature as the subcutaneous space of the recipient is not rich in blood vessels. Notably, frequent intravasation of tumor cells was observed in the primary sites (Fig. 2B), wherein the intravascular tumor cells always maintained their alveolar structure. Occasionally, tumor microemboli, covered with flat

Published OnlineFirst December 15, 2016; DOI: 10.1158/0008-5472.CAN-16-2486

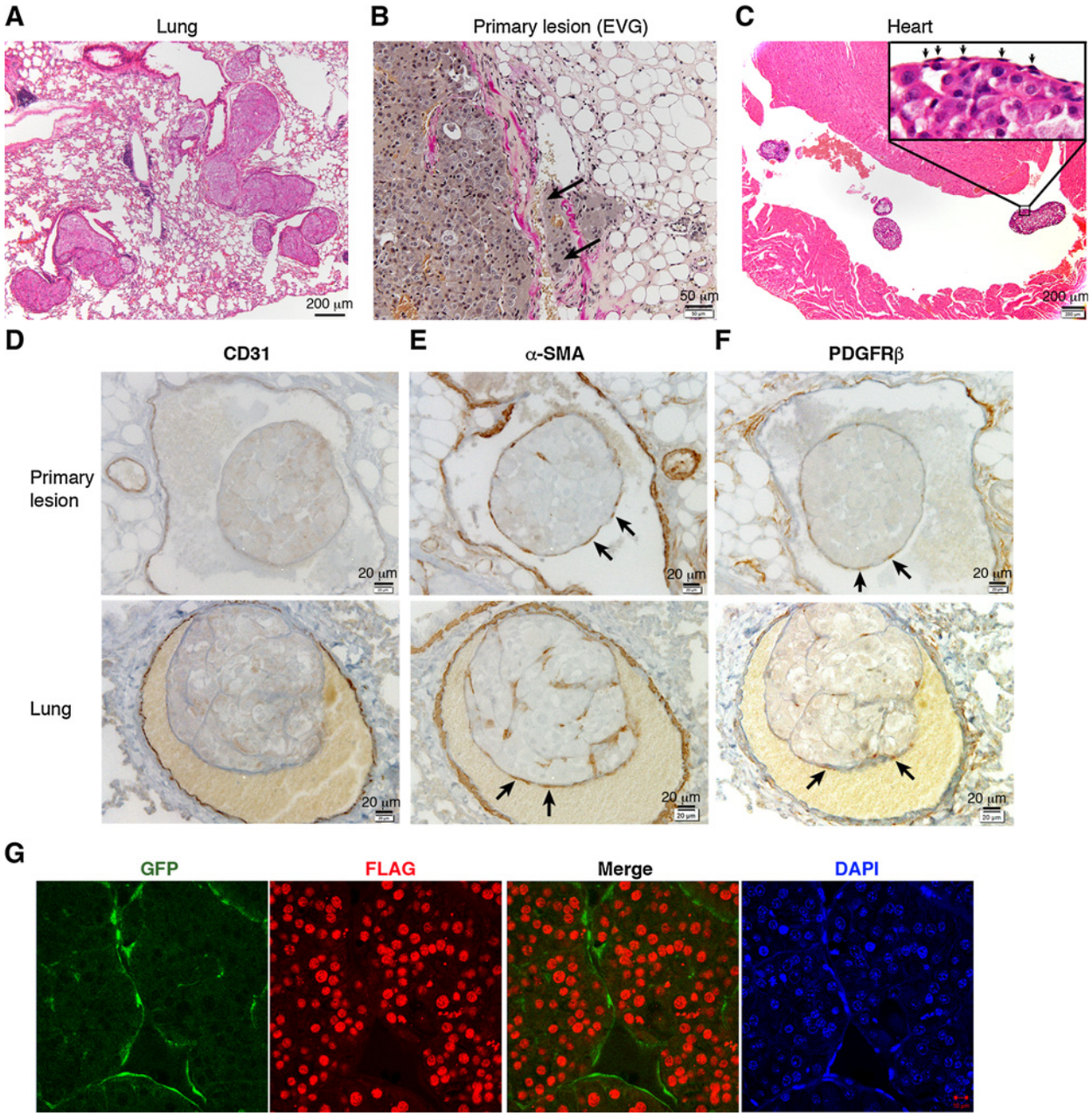

Figure 2.

Hematogenous metastasis of the murine ASPS. **A,** Multiple metastatic foci in the lung. H&E staining. **B,** Intravasation of tumor cells (arrows). Van Gieson's staining. **C,** Intracardiac tumor emboli. The inset shows the tumor organoid surrounded by flat epithelial–like cells (arrows), H&E staining. **D–E,** Immunohistochemical analysis of vascular markers CD31 (**D**), αSMA (**E**), and PDGFRB (**F**) for intravascular tumor cells in the primary lesion (top) and in the lung (bottom). **G,** Immunofluorescence assessment of cellular origins of the ASPS vascular network in GFP tg mice as recipients. Vascular cells of recipient origin are positive for GFP, whereas ASPS tumor cells are positive for FLAG but not for GFP.

epithelial–like cells (Fig. 2C), were seen in the right cardiac ventricle and were also observed as small alveolar organoids.

Immunostaining showed the presence of an abundant vascular network indicated as CD31-positive vascular endothelial cells (Fig. 1G). Intravascular tumor nests of both primary sites and lung metastases were covered with CD31-negative, aSMA-positive, and PDGFRB-positive hemangiopericytes (Fig. 2D–F). The hemangiopericytic cells surrounding intracardiac tumor emboli and intravascular tumor nests did not express FLAG-tagged ASPSCR1-TFE3, suggesting that they were of recipient origin (Supplementary Fig. S2A–S2C). Furthermore, when ASPS developed in recipient GFP transgenic mice, the vascular network was GFP-positive and FLAG-negative, distinct from the profile of tumor cells of Balb/c origin (Fig. 2G; Supplementary Fig. S2D).

Published OnlineFirst December 15, 2016; DOI: 10.1158/0008-5472.CAN-16-2486

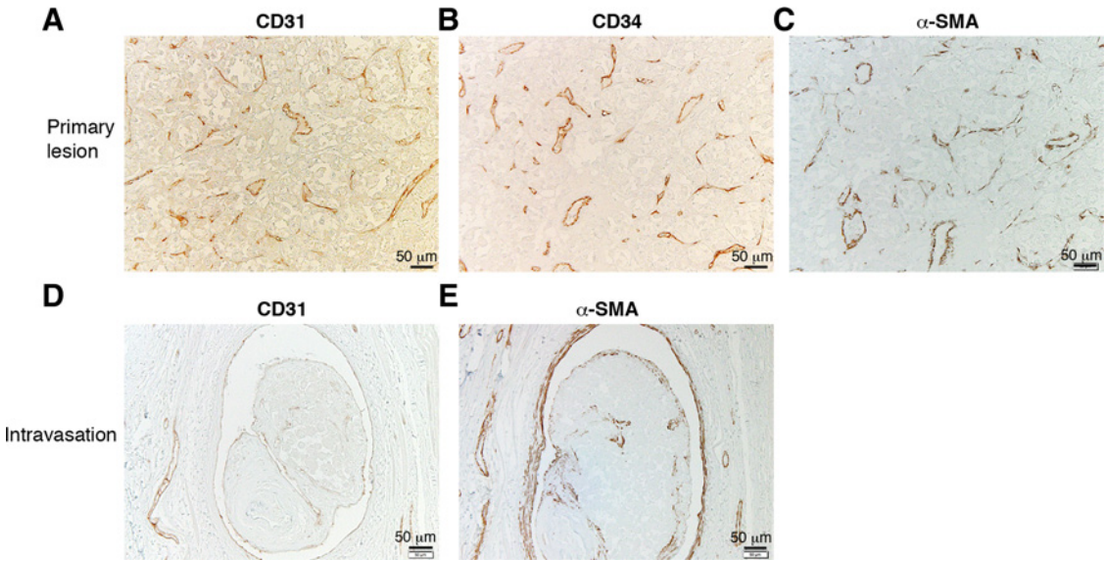

Figure 3.

Immunostaining of vascular markers in human ASPS. **A–C,** Primary tumor. CD31-positive (**A**) and CD34-positive (**B**) endothelial cells and aSMA-positive (**C**) hemangiopericytes could be observed in the vascular network. **D–E,** Tumor intravasation. CD31-positive endothelial cells are positive in the blood vessel but only partially positive in the tumor encapsulation (**D**). In contrast, the intravascular tumor organoid is constitutively covered with aSMA-positive hemangiopericytes (**E**).

Collectively, the results indicate that ASPS tumor cells efficiently attracted both hemangiopericytes and endothelial cells and that the intravascular tumor cells were covered and protected by hemangiopericytes.

The presence of hemangiopericytes in human ASPS was also examined immunohistochemically. CD31- and CD34-positive endothelial cells were enriched and accompanied by aSMA-positive hemangiopericytes (Fig. 3A–C). The intravascular tumor cell organoids were covered with both CD31-positive endothelial cells and aSMA-positive hemangiopericytes, although the latter were predominantly similar as seen in mouse ASPS (Fig. 3D and E). Collectively, the induction of hemangiopericytes appears to represent a common feature both in human and mouse ASPSs, and the encapsulation of tumor cells by hemangiopericytes comprises an important characteristics of intravascular tumor cells.

Expression profiles of mouse ASPS

To examine molecules and signaling pathways considered important for vasculogenesis, vascular invasion, and metastasis, gene expression profiles were compared between murine ASPS tumors and mouse normal tissue, and between eMCs introduced with the *ASPSCR1-TFE3* retrovirus or with an empty vector. The microarray analysis showed that 1,846 and 1,527 genes were upregulated in ASPS tumors versus normal tissue (fold change > 2.0) and in *ASPSCR1-TFE3*–expressing eMCs versus eMCs with an empty vector (fold change > 1.5), respectively. Furthermore, 697 genes were shown to be upregulated in both categories (Fig. 4A). It is considered possible that genes important for development, maintenance, vasculogenesis, and metastasis are included among the genes upregulated in ASPS tumors. In turn, genes upregulated both in ASPS and *ASPSCR1-TFE3*–expressing eMCs likely contain direct targets of ASPSCR1-TFE3 that are crucial in the early stage of tumor development. The lists of upregulated genes are shown in Supplementary Tables S2–S4, and the 17 genes upregulated both in ASPS- and eMCs-expressing *ASPSCR1-TFE3* that possess vasculogenic potentials or considered to play roles in invasion or metastasis are shown in Table 1. Of these, the upregulated expression of *Gpnmb*, *Kdelr3*, *Mdk*, *Ctsk*, and *Angptl2* in ASPS and eMCs was also confirmed by quantitative RT-PCR (Fig. 4B). In addition, 8 of 17 genes (*Gpnmb*, *Kdelr3*, *Mdk*, *Srpx2*, *Ctsk*, *Pgf*, *Angptl2*, and *Vegfb*) were found upregulated in human ASPS and/or patient-derived xenograft (5, 17, 18), indicating the reliability of our model.

GSEA showed strong correlation between gene expression in ASPS and the lysosome pathway (Fig. 4C). Specifically, the TFE/MITF proteins transregulate autophagy- and lysosomal-related genes, and this pathway is activated in human malignancies such as malignant melanoma and pancreatic cancer (19, 20). In addition, lysosomal regulation and subsequent metabolic reprogramming are also important genetic events in ASPS. These findings were also consistent with abundant lysosomes observed in murine ASPS cells (Supplementary Fig. S1B).

The systemic analysis of biological functions and signaling pathways for 697 genes upregulated in ASPS tumors and eMCs expressing *ASPSCR1-TFE3* was performed using the IPA. Significant involvement of phagosome and autophagy pathways, and disorders related to lysosomal dysfunction were highlighted, and association with gene regulation by the TFE/MITF family was confirmed (Fig. 4D; Supplementary Fig. S4).

Increased transendothelial migration of ASPS cells mediated by GPNMB upregulation

Substantive angiongenic activities and the induction of hemangiopericytes as important features of the initial stage of ASPS metastasis followed by intravasation of tumor cells were

Published OnlineFirst December 15, 2016; DOI: 10.1158/0008-5472.CAN-16-2486

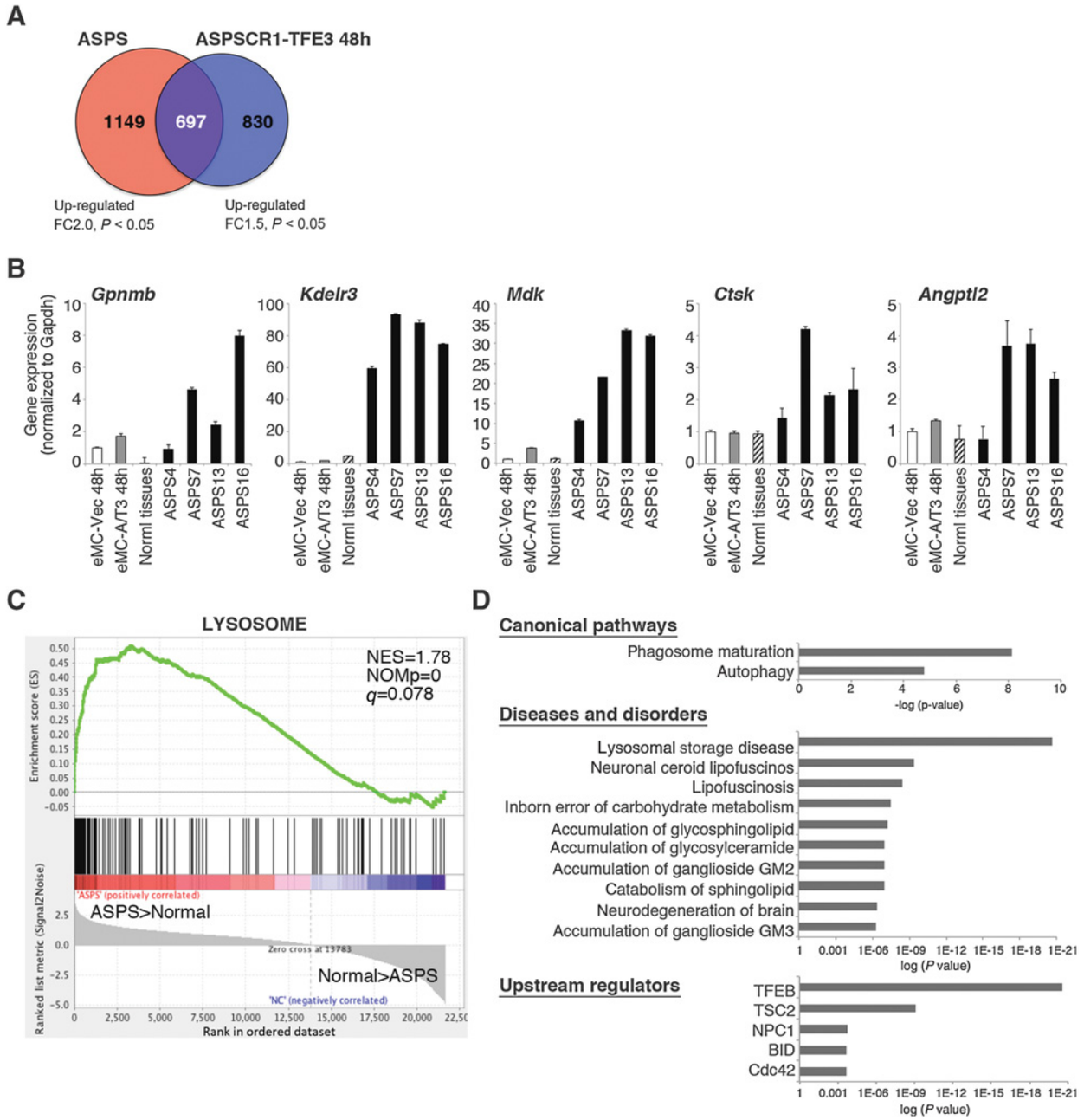

Figure 4.

Gene expression profiles of mouse ASPS tumors and eMCs expressing *ASPSCR1-TFE3*. **A,** Venn diagram showing upregulated genes in ASPS tumors ($n = 19$) versus the mixture of normal tissues and in eMCs expressing *ASPSCR1-TFE3* versus those containing an empty vector ($n = 4$, each). **B,** Real-time quantitative RT-PCR for *Gpnmb, Kdelr3, Mdk, Ctsk,* and *Angptl2* in eMCs with or without *ASPSCR1-TFE3* and in four independent ASPS tumors. Mean ± SEM is shown. **C,** GSEA of ASPS versus normal tissue shows enrichment of the gene set involved in lysosome function. **D,** Systematical analysis of the signaling pathways for 697 upregulated genes in ASPS tumors and eMC expressing *ASPSCR1-TFE3* (**A**) by the IPA software. The key canonical pathways, diseases and disorders, and upstream regulators are listed according to their ranking scores.

frequently observed both in human and mouse ASPS as previously described. The interaction between tumor cells and endothelial cells has been considered one of the key points for tumor intravasation (21), and we accordingly predicted that ASPS cells possess increased interactive and transmigratory activities against endothelial cells as well. To address this issue, we carried out a transendothelial migration assay. Briefly, immortalized CD31-positive and PDGFRB-negative hemangioendothelial cells originally purified from 18.5 dpc Balb/c mouse embryos were seeded onto Boyden chambers and

Published OnlineFirst December 15, 2016; DOI: 10.1158/0008-5472.CAN-16-2486

Table 1. Upregulated genes in ASPS and eMCs containing ASPSCR1-TFE3 potentially involved in vasculogenesis, tumor invasion, and/or metastasis

Gene name	FC in tumor[a]	FC in eMC[b]	Gene product
Gpnmb	50.08	2.30	Glycoprotein nmb
Kdelr3	25.82	2.05	KDEL endoplasmic reticulum protein retention receptor 3
Mdk	17.90	2.79	Midkine
Fgfbp3	13.04	12.42	Fibroblast growth factor binding protein 3
Srpx2	12.33	1.78	Sushi-repeat–containing protein, X-linked 2
Ctsk	9.78	2.07	Cathepsin K
Pgf	7.25	4.14	Placental growth factor
Angptl2	6.97	1.70	Angiopoietin-like 2
Cyba	4.66	2.85	Cytochrome b-245, alpha polypeptide
Rnh1	4.63	2.56	Ribonuclease/angiogenin inhibitor 1
Sfrp2	4.37	1.72	Secreted frizzled-related protein 2
Tgfb2	4.17	2.78	Transforming growth factor, beta 2
Efna3	3.45	1.72	Ephrin A3
Vegfb	3.23	1.68	Vascular endothelial growth factor B
Gna13	2.88	2.00	Guanine nucleotide binding protein, alpha 13
Dhcr7	2.15	1.70	7-dehydrocholesterol reductase
Nus1	2.05	1.65	Nuclear undecaprenyl pyrophosphate synthase 1

[a]Fold change (FC) of gene expression, ASPS versus normal tissue.
[b]FC of gene expression, eMCs-expressing *ASPSCR1-TFE3* versus those containing an empty vector.

irradiated to suppress proliferation and endogenous endothelial cell migration. Murine ASPS cells were then seeded, and migration with or without endothelial cells was assessed at 24 hours after seeding. Both ASPS and Ewing sarcoma cells (10) showed similar migratory activities in the absence of endothelial cells, whereas ASPS cells demonstrated significantly enhanced transendothelial migration (Fig. 5A).

As shown in Fig. 4 and Table 1, the glycoprotein nonmetastatic b/osteoactivin, gene (*Gpnmb*) was significantly upregulated both in mouse ASPS tumors and in eMCs expressing ASPSCR1-TFE3. GPNMB is a transmembrane glycoprotein that is known to be involved in tumor cell invasion and metastasis of multiple cancer types (22–24). *Gpnmb* overexpression induces tumor invasiveness, endothelial cell migration, and transendothelial migration of cancer cells (20, 25). In accordance with our gene expression data, *Gpnmb* has been reported as a transcriptional target of MITF and TFE3 in renal cancer cells (26), suggesting that Gpnmb represents one of the key downstream molecules of ASPSCR1-TFE3 responsible for ASPS invasion and metastasis.

In support of this key role, we found that GPNMB was expressed in all cases of mouse and human ASPS examined using immunostaining. In addition, enhanced GPNMB staining was evident at the front of tumor invasion and intravascular tumor foci (Fig. 5B–E). Our data and the proposed roles of GPNMB in cancer invasion and metastasis further suggest that GPNMB is crucial for the interaction between ASPS tumor cells and endothelial cells to initiate metastasis. Consistent with this function, the transendothelial migration activity was inhibited by siRNA-mediated knockdown of *Gpnmb* (Fig. 5F), indicating that *Gpnmb* expression is required for intravasation of ASPS cells.

The *ASPSCR1* fusion gene–expressing *ex vivo* model defines tumorigenic activity of the C-terminal domains in TFE/MITF family proteins

TFE3 belongs to the TFE/MITF transcription protein family, which has been found to be involved in human cancer and within which the DNA binding bHLH leucine zipper motif is well conserved (27). TFE3 is fused to ASPSCR1 and several other genes in renal cell carcinoma, whereas TFEB is a component of fusion genes in a minor proportion of renal cell carcinoma cases (28–31). Mitf plays an important role in the survival and maintenance of malignant melanoma (32). The involvement of TFE/MITF family proteins in human cancer suggests the presence of common and/or distinct functional motifs in their C-terminal regions. The functional heterogeneity and common property of these regions in tumorigenesis can be evaluated as the oncogenic activities of ASPSCR1 fusion genes in our model system.

To examine the oncogenic activity of ASPSCR1 fusion genes, artificial chimeric genes were generated consisting of the 5′ ASPSCR1 and 3' TFE/MITF sequences. Tumorigenic activities of eMCs expressing each fusion gene were examined. The Kaplan–Meier survival curve indicated that *ASPSCR1-TFE3* and *ASPSCR1-TFEB* but not *ASPSCR1-TFEC* and *ASPSCR1-MITF* induced sarcoma (Fig. 6A). Notably, recipients transplanted with *ASPSCR1-TFEB* developed sarcoma following a significantly longer latency ($P < 0.001$ by log-rank test); however, the morphology of *ASPSCR1-TFEB*–expressing tumors was very similar with that of *ASPSCR1-TFE3*–expressing ASPS (Fig. 6B and C). These results suggest the existence of common functional domains between TFE3 and TFEB C-termini and that the motif is lacking in TFEC and MITF. In addition, the tumorigenic activity of *ASPSCR1-TFEB* was weaker than that of *ASPSCR1-TFE3*. Together, these findings will be helpful toward identifying novel important functional motifs for tumorigenesis in TFE/MITF family protein and cofactors of ASPSCR1-TFE3.

Discussion

Our novel model for human ASPS exhibited high incidence of spontaneous metastasis to the lung. To acquire such high metastatic potentials, the ASPS model exhibited characteristic behaviors at several different steps of the metastatic process: (1) strong angiogenic activity mediated by the induction of hemangiopericytes, (2) frequent tumor intravasation, and (3) organoid structures covered with hemangiopericytes in the blood stream. Notably, these findings are also observed in human ASPS (1–3); thus, our model provides important information for clarifying the metastatic mechanisms of ASPS.

Published OnlineFirst December 15, 2016; DOI: 10.1158/0008-5472.CAN-16-2486

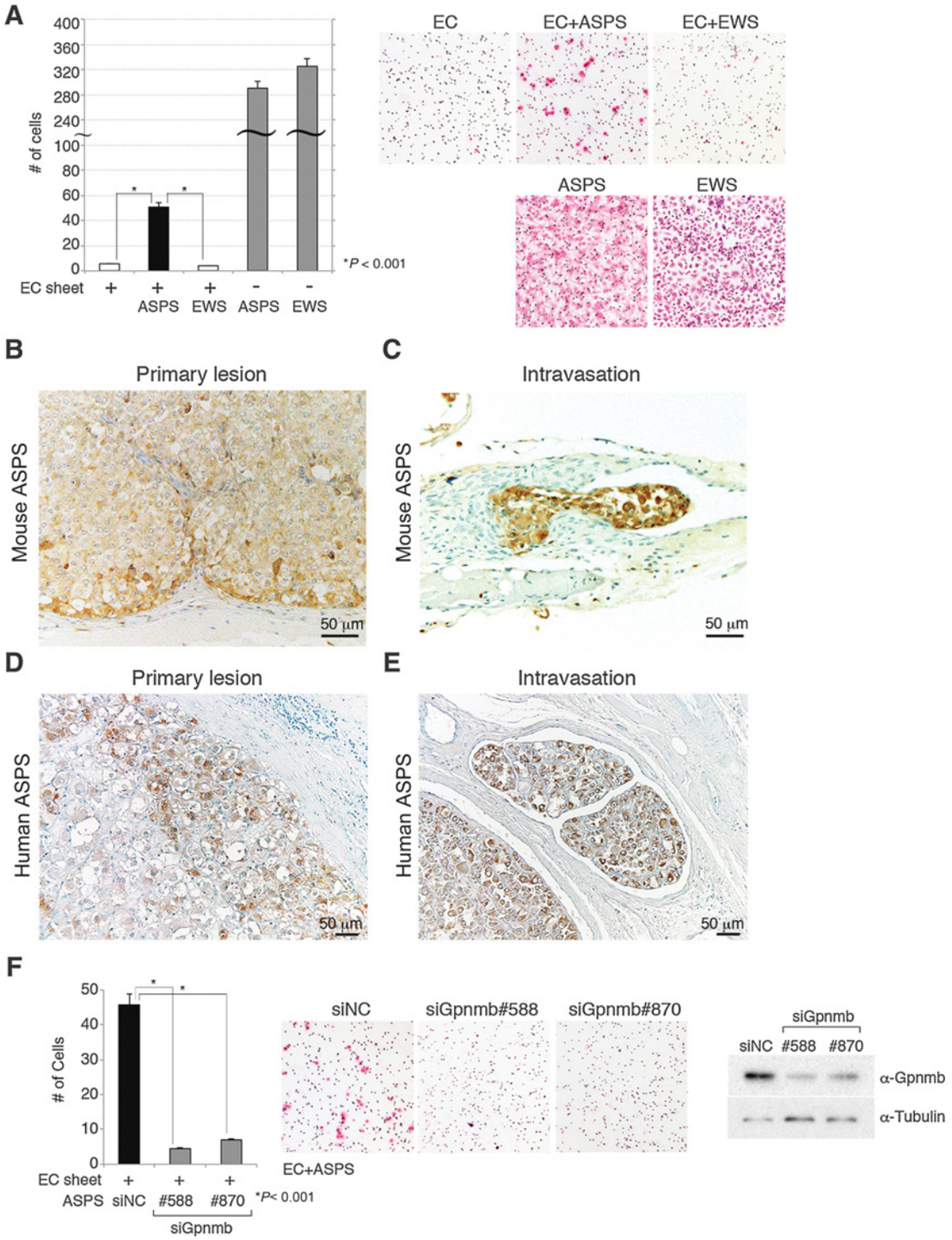

Figure 5.

Enhanced transendothelial migration and *Gpnmb* expression in ASPS. **A,** Boyden chamber assay showing enhanced transendothelial migration of ASPS compared with Ewing sarcoma cells assessed by the number of migrated cells (left). H&E staining of migrated cells is shown in the right plots. Data represent mean ± SEM of three independent experiments. *, $P < 0.001$. **B–E,** Immunostaining of GPNMB in mouse (**B** and **C**) and human (**D** and **E**) ASPS. GPNMB staining is enhanced at the front of tumor invasion (**B** and **D**) and intravasation (**C** and **E**). **F,** siRNA-mediated gene silencing of *Gpnmb* inhibited transendothelial migration of ASPS as shown in the cell numbers (left) and microscopic images (middle). The efficiency of *Gpnmb* silencing is shown by Western blotting (right). Two independent siRNAs, #588 and #870, were used. Data represent mean ± SEM of three independent experiments. *, $P < 0.001$.

Published OnlineFirst December 15, 2016; DOI: 10.1158/0008-5472.CAN-16-2486

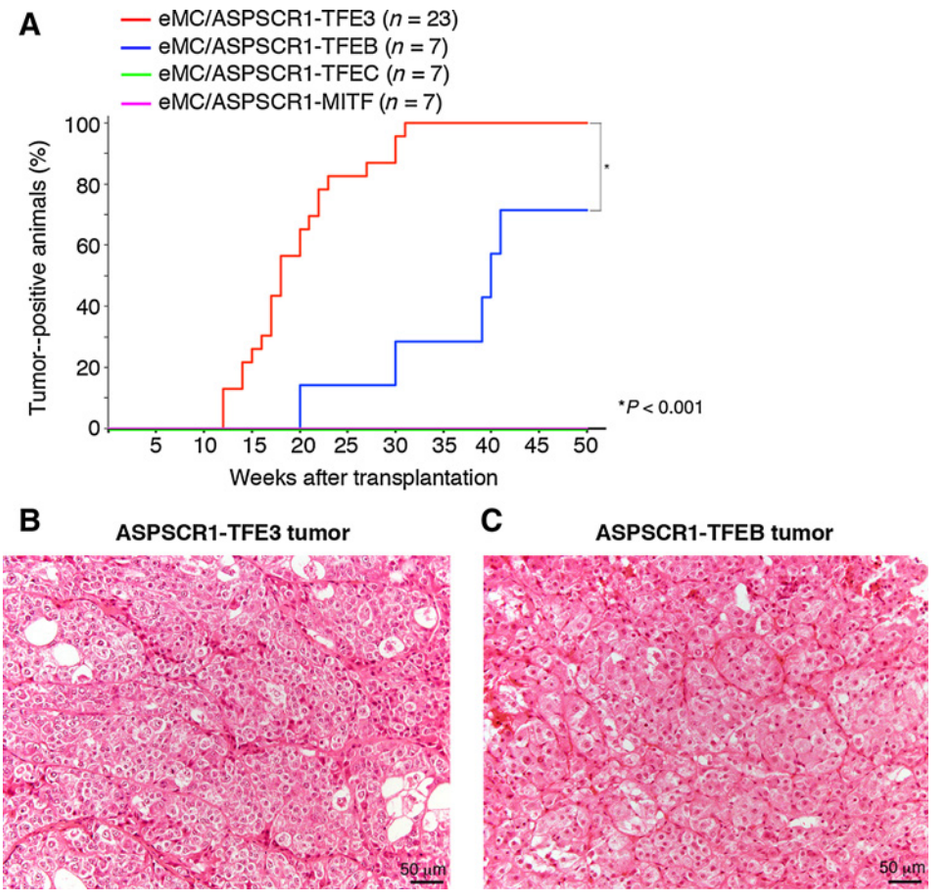

Figure 6.
Tumor development by eMCs expressing *ASPSCR1* fusion genes. **A,** Cumulative incidence of ASPS-like tumors. In three mutants, only *ASPSCR1-TFEB*–expressing eMCs induced tumors in nude mice, exhibiting significantly longer latency than that shown by *ASPSCR1-TFE3*–expressing eMCs ($P < 0.001$ by log-rank test). **B** and **C,** Morphologies of *ASPSCR1-TFE3*–induced (**B**) and *ASPSCR1-TFEB*–induced (**C**) tumors.

Tumor angiogenesis is often incomplete and lacks a hemangiopericytic lining, resulting in leakage and insufficient oxygen supply (33). In contrast, the tumor-associated vessels in ASPS are accompanied by hemangiopericytes and/or smooth muscle cells that completely cover the vessel wall as was shown in our present study. In addition, ASPS shows very limited areas of necrosis even when the tumor grows up to a large mass. These findings suggest that ASPS tumor cells attract hemangiopericyte migration and/or proliferation by secreting bioactive substances. Experiments to identify such molecules are currently underway using human and mouse ASPS cells and purified hemangiopericytes.

The hemangiopericytic capsule surrounding the tumor cells in the blood vessels represents an unanticipated phenomenon that was observed in both human and mouse ASPS. It is likely that hemangiopericytic encapsulation protects tumor cells from attack by the host immune system in the blood stream. Consistent with this suggestion, when mouse ASPS cell suspensions were injected into the mouse tail vein, they failed to show pulmonary metastasis despite high metastatic activity from the subcutaneous tumor (data not shown). These data indicate that the inhibition of hemangiopericyte induction in ASPS might represent a novel, powerful, and promising strategy for the treatment and prevention of metastasis.

The ASPSCSR1-TFE3/Gpnmb axis plays a key role in the intravascular invasion of ASPS cells, as was indicated by the strong expression of GPNMB in the intravascular lesions and by the results following gene silencing of *Gpnmb* in a transendothelial migration experiment. *Gpnmb* functions as a transcriptional target of TFE/MITF family transcription factors (26) and was found to be upregulated by *ASPSCSR1-TFE3* expression in this study. The observation of stronger expression of the GPNMB protein at the invasion front and intravasation suggests that there might be additional signals or posttranslational modification reinforcing the effect of transactivation by ASPSCR1-TFE3. As clinical trials of antibody drugs for GPNMB are in progress for multiple human cancer types (34), ASPS may also represent a good target for the antibody therapy targeting GPNMB.

The gene set for lysosome and autophagy function was upregulated in our ASPS model along the identification of abundant lysosomes in tumor cells. TFE/MITF transcription factors promote lysosomal functions in many cell types and cancer; in turn, these functions are modulated by other signaling pathways such as mTORC1 and Wnt (31, 35, 36). The results of the current study suggest that the chimeric ASPSCR1-TFE3 protein may retain or even increase the accessibility to lysosomes (35), and may therefore function as a nutrient sensor. In this context, it is notable that increased lactate uptake was reported in another murine ASPS model (9), as ASPS may actively utilize abnormal nutrient and metabolic conditions in the tumor microenvironment. Nevertheless, the previous knock-in model for ASPS lacks metastatic properties (9). Although the cause of phenotypic differences between two models remains unclear, the origins of *ASPSCR1-TFE3*–expressing cell might be critical to obtain proper ASPS phenotypes.

Furthermore, using our novel *ex vivo* mouse model, we could directly evaluate the oncogenic activity of *ASPSCR1* fusion genes. Our system proved quite useful to define the important motif in TFE/MITF proteins. Specifically, in three members of TFE/MITF family proteins other than TFE3, oncogenic potential was found only in TFEB when its C-terminus was fused to ASPSCR1. This result is consistent with the demonstrated involvement of TFEB in genetic fusions of renal cell carcinoma (31). However, our result indicates that the tumor incidence was lower and the latency was longer in the *ASPSCR1-TFEB* cohort than those in the *ASPSCR1-TFE3* cohort, which may explain the reason why *ASPSCR1-TFEB* has not been identified in ASPS. Studies to identify the important motif in the TFE3 C-terminus and putative cofactors that may bind to this motif are in progress.

In conclusion, hematogenous metastasis is the most important factor in determining the prognosis of patients with ASPS. The present model faithfully recapitulates human ASPS with respect to its characteristic vascular networking, vascular invasion, and metastasis. Thus, this model provides useful information to clarify the oncogenic and metastatic mechanisms of not only ASPS but potentially of other cancers having similar vascular networks such as renal cell carcinoma.

Disclosure of Potential Conflicts of Interest

No potential conflicts of interest were disclosed.

Authors' Contributions

Conception and design: M. Tanaka, T. Nakamura
Development of methodology: M. Tanaka, T. Nakamura
Acquisition of data (provided animals, acquired and managed patients, provided facilities, etc.): M. Tanaka, M. Homme, Y. Yamazaki, R. Shimizu, Y. Takazawa, T. Nakamura
Analysis and interpretation of data (e.g., statistical analysis, biostatistics, computational analysis): M. Tanaka, R. Shimizu, T. Nakamura
Writing, review, and/or revision of the manuscript: M. Tanaka, M. Homme, Y. Yamazaki, R. Shimizu, Y. Takazawa, T. Nakamura
Administrative, technical, or material support (i.e., reporting or organizing data, constructing databases): Y. Takazawa, T. Nakamura
Study supervision: M. Tanaka, T. Nakamura

Acknowledgments

The authors thank Dr. Mitsuyoshi Kato and Dr. Eirikur Steingrimsson for helpful suggestions, and Yoshiko Yamazaki for technical assistance.

Grant Support

The study was supported by Grants-in-Aid for Scientific Research from Japan Society for the promotion of science (nos. 26250029 to T. Nakamura and 16K07131 to M. Tanaka).

The costs of publication of this article were defrayed in part by the payment of page charges. This article must therefore be hereby marked *advertisement* in accordance with 18 U.S.C. Section 1734 solely to indicate this fact.

Received September 9, 2016; revised November 5, 2016; accepted November 21, 2016; published OnlineFirst December 15, 2016.

References

1. Zarrin-Khameh N, Kaye KS. Alveolar soft part sarcoma. Arch Pathol Lab Med 2007;131:488–91.
2. Fisher C. Soft tissue sarcomas with non-EWS translocations: Molecular genetic features and pathologic and clinical correlations. Virchows Arch 2010;456:153–66.
3. Folpe AL, Deyrup AT. Alveolar soft-part sarcoma: A review and update. J Clin Pathol 2006;59:1127–32.
4. Ladanyi M, Lui MY, Antonescu CR, Krause-Boehm A, Meindl A, Argani P, et al. The der(17)t(X;17)(p11;q25) of human alveolar soft part sarcoma fuses the TFE3 transcription factor gene to ASPL, a novel gene at 17q25. Oncogene 2001;20:48–57.
5. Stockwin LH, Vistica DT, Kenney S, Schrump DS, Butcher DO, Raffeld M, et al. Gene expression profiling of alveolar soft-part sarcoma (ASPS). BMC Cancer 2009;9:22
6. Covell DG, Wallqvist A, Kenney S, Vistica DT. Bioinformatic analysis of patient-derived ASPS gene expressions and ASPL-TFE3 fusion transcript levels identify potential therapeutic targets. PLoS One 2012;7:e48023.
7. Selvarajah S, Pyne S, Chen E, Sompallae R, Ligon AH, Nielsen GP, et al. High-resulution array CGH and gene expression profiling of alveolar soft part sarcoma. Clin Cancer Res 2014;20:1521–30.
8. Lazar AJF, Das P, Tuvin D, Korchin B, Zhu Q, Jin Z, et al. Angiogenesis-promoting gene patterns in alveolar soft part sarcoma. Clin Cancer Res 2007;13:7314–21.
9. Goodwin ML, Jin H, Strasessler K, Smith-Fry K, Zhu JF, Monument MJ, et al. Modeling alveolar soft part sarcomagenesis in the mouse: A role for lactate in the tumor microenvironment. Cancer Cell 2014;26:851–62.
10. Tanaka M, Yamazaki Y, Kanno Y, Igarashi K, Aisaki K, Kanno J, et al. Ewing's sarcoma precursors are highly enriched in embryonic osteochondrogenic progenitors. J Clin Invest 2014;124:3061–74.
11. Okabe M, Ikawa M, Kominami K, Nakanishi T, Nishimune Y. `Green mice' as a source of ubiquitous green cells. FEBS Lett 1997;407:313–9.
12. Dar A, Domev H, Ben-Yosef O, Tzukerman M, Zeevi-Levin N, Novak A, et al. Multipotent vasculogenic pericytes from human pluripotent stem cells promote recovery of murine ischemic limb. Circulation 2012;125:87–99.
13. Hooper S, Marshall JF, Sahai E. Tumor cell migration in three dimensions. Methods Enzymol 2006;406:625–43.
14. Kawamura-Saito M, Yamazaki Y, Kaneko K, Kawaguchi N, Kanda H, Mukai H, et al. Fusion between CIC and DUX4 up-regulates PEA3 family genes in Ewing-like sarcomas with t(4;19)(q35;q13) translocation. Hum Mol Genet 2006;15:2125–37.
15. Yokoyama T, Nakatake M, Kuwata T, Couzinet A, Goitsuka R, Tsutsumi S, et al. MEIS1-mediated transactivation of synaptotagmin-like 1 promotes CXCL12/CXCR4 signaling and leukemogenesis. J Clin Invest 2016;126:1664–78.
16. Subramanian A, Kuehn H, Gould J, Tamayo P, Mesirov JP. GSEA-P: A desktop application for gene set enrichment analysis. Bioinformatics 2007;23:3251–3.
17. Vistica DT, Hollingshead M, Borgel SD, Kenney S, Stockwin LH, Raffeld M, et al. Therapeutic vulnerability of an in vivo model of alveolar soft part sarcoma (ASPS) to anti-angiogenic therapy. J Pediatr Hematol Oncol 2009;31:561–70.
18. Kenney S, Vistica DT, Stockwin LH, Burkett S, Hollingshead MG, Borgel SD, et al. ASPS-1, a novel cell line manifesting key features of alveolar soft part sarcoma. J Pediatr Hematol Oncol 2011;33:360–8.
19. Ploper D, Taelman VF, Robert L, Perez BS, Titz B, Chen HW, et al. MITF drives endolysosomal biogenesis and potentiates Wnt signaling in melanoma cells. Proc Natl Acad Sci USA 2015;112:E420–9.
20. Perera RM, Stoykova S, Nicolay BN, Ross KN, Fitamant J, Boukhali M, et al. Transcriptional control of autophagy-lysosome function drives pancreatic cancer metabolism. Nature 2015;524:361–5.
21. Reymond N, d'Agua BB, Ridley AJ. Crossing the endothelial barrier during metastasis. Nat Rev Cancer 2013;13:858–70.
22. Maric G, Rose AA, Annis MG, Siegel PM. Glycoprotein non-metastatic b (GPNMB): A metastatic mediator and emrging therapeutic target in cancer. Onco Targets Ther 2013;6:839–52.
23. Rose AA, Grosset AA, Dong Z, Russo C, Macdonald PA, Bertos NR, et al. Glycoprotein nonmetastatic B is an independent prognostic indicator of recurrence and a novel therapeutic target in breast cancer. Clin Cancer Res 2010;16:2147–56.
24. Kuan CT, Wakiya K, Dowell JM, Hemdon JE 2nd, Reardon DA, Graner MW, et al. Glycoprotein nonmetastatic melanoma protein B, a potential molecular therapeutic target in patients with glioblastoma multiforme. Clin Cancer Res 2006;12:1970–82.
25. Rose AA, Pepin F, Russo C, Abou Khalil JE, Hallett M, Siegel PM. Osteoactivin promotes breast cancer metastasis to bone. Mol Cancer Res 2007;5:1001–14.

26. Hong SB, Oh HB, Valera VA, Baba M, Schmidt LS, Linehan WM. Inactivation of the FLCN tumor suppressor gene induces TFE3 transcriptional activity by increasing its nuclear localization. PLoS One 2010;5:e15793.
27. Steingrimsson E, Tessarollo L, Pathak B, Hou L, Arnheiter H, Copeland NG, et al. Mitf and Tfe3, two members of the Mitf-Tfe family of bHLH-Zip transcription factors, have important but functionally redundant roles in osteoclast development. Proc Natl Acad Sci USA 2002;99:4477–82.
28. Sidhar SK, Clark J, Gill S, Hamoudi R, Crew AJ, Gwilliam R, et al. The t(X;1)(p11.2;q21.2) translocation in papillary renal cell carcinoma fuses a novel gene PRCC to the TFE3 transcription factor gene. Hum Mol Genet 1996;5:1333–8.
29. Argani P, Antonescu CR, Illei PB, Lui MY, Timmons CF, Newbury R, et al. Primary renal neoplasms with the ASPL-TFE3 gene fusion of alveolar soft part sarcoma: A distinctive tumor entity previously included among renal cell carcinomas of children and adolescents. Am J Pathol 2001;159:179–92.
30. Komai Y, Fujiwara M, Fujii Y, Mukai H, Yonese J, Kawakami S, et al. Adult Xp11 translocation renal cell carcinoma diagnosed by cytogenetics and immunohistochemistry. Clin Cancer Res 2009;15:1170–6.
31. Davis IJ, His BL, Arroyo JD, Vargas SO, Yeh YA, Motyckova G, et al. Cloning of an Alph-TFEB fusion in renal tumors harboring the t(6;11)(p21;q13) chromosome translocation. Proc Natl Acad Sci USA 2003;100:6051–6.
32. McGill GG, Horstmann M, Wildlund HR, Du J, Motyckova G, Nishimura EK, et al. Bcl2 regulation by the melanocyte master regulator Mitf modulates lineage survival and melanoma cell viability. Cell 2002;109:707–16.
33. Morikawa S, Baluk P, Kaidoh T, Haskell A, Jain RK, McDonald DM. Abnormalities in pericytes on blood vessels and endothelial sprouts in tumors. Am J Pathol 2002;160:985–1000.
34. Yardley DA, Weaver R, Melisko ME, Saleh MN, Arena FP, Forero A, et al. EMERGE: A randomized phase II study of the antibody-drug conjugate glembatumumab vedotin in advanced glycoprotein NMB-expressing breast cancer. J Clin Oncol 2015;33:1609–19.
35. Roczniak-Ferguson A, Petit CS, Froehlich F, Qian S, Ky J, Angarola B, et al. The transcription factor TFEB links mTORC1 signaling to transcriptional control of lysosome homeostasis. Sci Signal 2012;5:ra42.
36. Martina JA, Diab HI, Lishu L, Jeong-A L, Patange S, Raben N, et al. The nutrient-responsive transcription factor TFE3 promotes autophagy, lysosomal biogenesis, and clearance of cellular debris. Sci Signal 2014;7:ra9.

Published OnlineFirst December 15, 2016; DOI: 10.1158/0008-5472.CAN-16-2486

Cancer Research
The Journal of Cancer Research (1916–1930) | The American Journal of Cancer (1931–1940)

AACR American Association for Cancer Research

Modeling Alveolar Soft Part Sarcoma Unveils Novel Mechanisms of Metastasis

Miwa Tanaka, Mizuki Homme, Yukari Yamazaki, et al.

Cancer Res 2017;77:897-907. Published OnlineFirst December 15, 2016.